Localized Dictionaries Based Orientation Field Estimation for Latent Fingerprints

Xiao Yang, *Student Member, IEEE,* Jianjiang Feng, *Member, IEEE,* and Jie Zhou, *Senior Member, IEEE*

Abstract—Dictionary based orientation field estimation approach has shown promising performance for latent fingerprints. In this paper, we seek to exploit stronger prior knowledge of fingerprints in order to further improve the performance. Realizing that ridge orientations at different locations of fingerprints have different characteristics, we propose a localized dictionaries-based orientation field estimation algorithm, in which noisy orientation patch at a location output by a local estimation approach is replaced by real orientation patch in the local dictionary at the same location. The precondition of applying localized dictionaries is that the pose of the latent fingerprint needs to be estimated. We propose a Hough transform-based fingerprint pose estimation algorithm, in which the predictions about fingerprint pose made by all orientation patches in the latent fingerprint are accumulated. Experimental results on challenging latent fingerprint datasets show the proposed method outperforms previous ones markedly.

Index Terms—Fingerprint enhancement, latent fingerprint matching, orientation field, dictionary, pose estimation, Hough transform, Markov random field

1 Introduction

Latent fingerprints refer to the impressions of fingers left on objects or surfaces. Such impressions are usually not directly visible unless some physical or chemical techniques are used to enhance them [1]. Latent fingerprints are very important evidence for law enforcement agencies to identify criminals and terrorists. Because of the very low image quality, features (such as minutiae) in latents are routinely marked by trained latent examiners so that they can be matched by automated fingerprint identification systems (AFIS) [2]. In recent years, however, the need for "lights out" latent identification is rapidly increasing because of the increasing number of latent matching transactions [3]–[5].

To fulfill "lights out" latent identification, robust latent enhancement techniques are indispensable. A very successful and popular fingerprint enhancement method is based on contextual filtering [8]–[12]. Given correct local ridge orientations and frequencies, contextual filtering can successfully connect broken ridges and separate joined ridges. But correct ridge orientation field is critical for the success of this method.

Conventional orientation field estimation methods estimate local ridge orientation by analyzing pixel values in very small neighborhood (say, 32×32 pixels), which are very sensitive to image noise. As shown in Fig. 1(b), the orientation field estimated by the well-known Short Time Fourier Transform (STFT) method [6] for a poor quality latent fingerprint is very noisy, containing many local orientation patches which are not likely to appear in real fingerprints. Such errors are analogous to the non-word errors in spelling correction [13]. To address the problem, prior knowledge of fingerprint orientation fields has been taken into account in [7]. A number of orientation patches extracted from real fingerprints are clustered to form a dictionary and noisy orientation patches are replaced by closest real orientation patches in the dictionary. As we can see from Fig. 1(c), the use of prior knowledge (in the form of orientation patch dictionary) is helpful for correcting many non-word errors. However, since the positions of the patches have not been restrained, some orientation patches may occur at impossible location. For example, the orientation field estimated by this algorithm for the latent in Fig. 1 contains a wrong delta singularity in the top region, which is not likely to occur in real fingerprints. Such errors are analogous to the real word errors in spelling correction [13]. These errors remind us that location-dependent prior knowledge of fingerprints should be exploited in orientation field estimation.

However, to exploit location-dependent prior knowledge in orientation field estimation, fingerprints need to be registered into a universal coordinate system, which itself is a challenging problem for poor quality fingerprints. Existing fingerprint registration approaches based on singular point [14] or point of maximum curvature [15] are sensitive to noise and can not be used if the corresponding area is very noisy or not available. But experienced fingerprint examiners can still roughly predict the pose of very incomplete and poor quality fingerprints such as those in Fig. 2. This fact suggests us that to achieve robust fingerprint registration, the statistics of whole orientation fields should be utilized.

In this paper, we propose a robust fingerprint registration algorithm, which is based on probabilistic

• *The authors are with the Department of Automation, Tsinghua University, Beijing 100084, China.*
E-mail: xiao-yang09@mails.tsinghua.edu.cn; {jfeng, jzhou}@tsinghua.edu.cn.

Manuscript received 30 Jan. 2013; revised 1 Aug. 2013; accepted 15 Sep. 2013. Date of current version 29 Apr. 2014.
Recommended for acceptance by D. Maltoni.
For information on obtaining reprints of this article, please send e-mail to: reprints@ieee.org, and reference the Digital Object Identifier below.
Digital Object Identifier 10.1109/TPAMI.2013.184

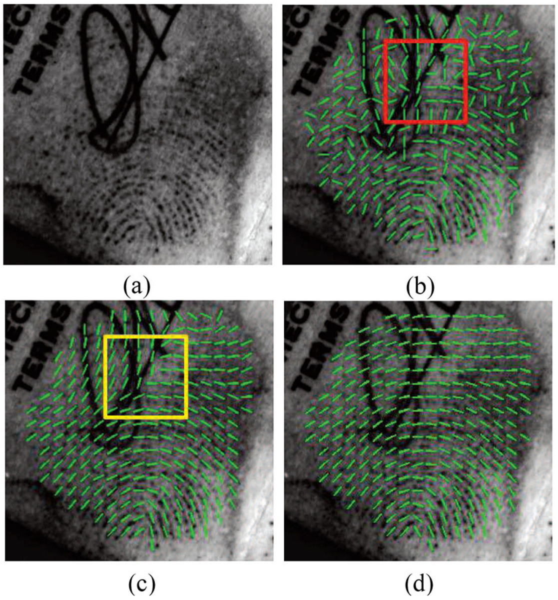

Fig. 1. Comparison of orientation fields of a latent fingerprint in: (a) Extracted by three different algorithms; (b) Short time Fourier transform in [6]; (c) Global dictionary-based approach in [7]; and (d) Proposed localized dictionary-based approach. The orientation field in (b) contains a lot of non-word errors as marked by the red box, while the orientation field in (c) contains real word errors as marked by the yellow box. Neither of the two types of errors is present in the orientation field in (d).

voting of all local orientation patches, and a robust fingerprint orientation field estimation algorithm, which is based on localized dictionaries of orientation patches. The outline of the whole system is shown in Fig. 3. Both the registration algorithm and the orientation field estimation algorithm consist of an off-line learning module and an on-line estimation module. In the offline learning stage, the spatial distributions of a set of prototype fingerprint orientation patches and a set of localized dictionaries of orientation patches are learnt based on a set of registered training orientation fields. Given an input fingerprint, the online estimation stage consists of the following steps:

1) An initial orientation field is estimated using local Fourier analysis.
2) The pose of the fingerprint is estimated using a probabilistic voting algorithm which is based on the spatial distributions of prototype orientation patches.
3) Candidate orientation patches are found for each patch in the registered initial orientation field by looking up the localized dictionaries.
4) The final orientation field is determined based on context information.

Extensive experiments on three latent fingerprint databases (NIST SD27 latent fingerprint database, Hisign latent fingerprint database, and Tsinghua overlapped latent fingerprint database) show that the proposed algorithm significantly outperforms representative algorithms published in the literature. The proposed algorithm has also been tested on the FVC-onGoing FOE benchmark and ranked first on the bad quality dataset.

Fig. 2. Latent fingerprints whose central areas are not available.

The rest of this paper is organized as follows. In section 2, published orientation field estimation methods and fingerprint pose estimation algorithms are reviewed. After that probabilistic voting based fingerprint pose estimation is detailed in section 3 and the localized dictionaries based orientation field estimation algorithm is introduced in section 4. Then, section 5 reports the experimental results and finally our work is summarized and potential research directions are discussed in section 6.

2 Related Work and Motivations

2.1 Orientation Field Estimation

Most fingerprint orientation field estimation approaches consist of two steps: local estimation, followed by regularization (or smoothing). In this subsection, we provide a brief review of representative approaches of each step and describe the motivation of our approach. For a more comprehensive review and a performance evaluation of existing orientation field estimation approaches, interested readers can refer to [16], [17].

2.1.1 Local Estimation

Gradient-based, slit-based, and local Fourier analysis are the three most widely used local estimation approaches. Gradient-based approaches compute pixelwise gradients and estimate local ridge orientation based on the gradients of local neighborhood [14], [18]–[20]. Slit-based approaches analyze the intensity variances along a set of orientations and choose the best orientation according to some measures [21], [22]. Local Fourier analysis approaches compute the Fourier transform of local fingerprint image and estimate dominant ridge orientation by analyzing the magnitude spectrum [6], [23]. Since these local orientation field estimation algorithms take only local image block into account, they will generate very noisy orientation fields in the case of poor quality fingerprints.

2.1.2 Regularization Based on Local Smoothness Assumption

A simple fact is that ridge orientations of fingerprint do not change abruptly in most regions. Several orientation field regularization approaches are based on this local smoothness assumption. Low-pass filtering based method [14] is the most commonly used smoothing method. A problem with this approach is that it is difficult to choose a proper size of the filtering window. To resolve the problem, multi-resolution orientation fields are used in several approaches [15], [22], [24]. However, such approaches cannot handle the cases where the initial orientation field is

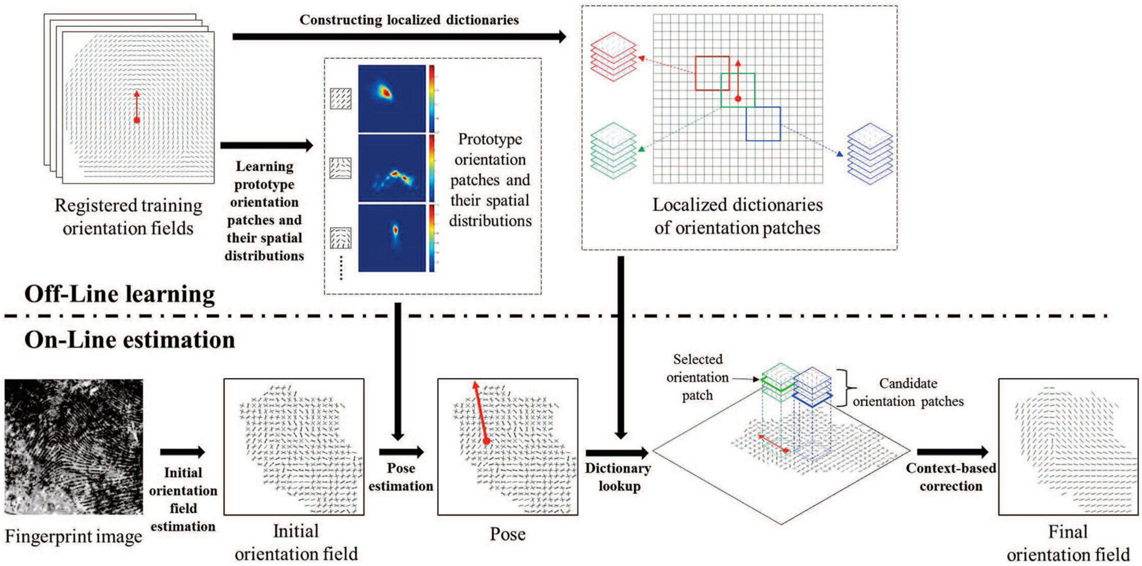

Fig. 3. Flowchart of the proposed fingerprint pose estimation and orientation field estimation approach. The approach is composed of two relatively independent parts. The first part is the off-line learning algorithm, while the second part is the on-line estimation algorithm.

significantly different from the true orientation field. Other commonly used smoothing methods are based on Markov random field (MRF) models [11], [25], [26] and variational approaches [27]. These approaches cannot deal with very poor quality fingerprints either, since they are also based on the simple local smoothness assumption.

2.1.3 Regularization Based on Surface Fitting

Some researchers view orientation field regularization as a surface fitting problem and use general functions, such as, polynomials [28]–[30] and Fourier series [31], to represent fingerprint orientation fields. To address the special discontinuity pattern of singular region, several specific models are proposed, such as the zero-pole model [32], point-charge model [33], [34], phase portrait model [35] and quadratic differentials [36]. However, these models are quite general in the sense that they can represent arbitrary orientation fields. Without any constraint on the valid range of parameters, these approaches will generate invalid fingerprint orientation fields in the case of severe noise. An additional inconvenience with the models which require explicit information of singular points is that singular point detection in latents itself is a very difficult problem. That is why manually marked singular points were used in the latent enhancement algorithms in [37], [38].

2.1.4 Regularization Based on Dictionary Lookup

Orientation field regularization using a dictionary of real orientation patches is proposed in [7]. This method uses an orientation patch dictionary constructed from a set of real fingerprint orientation fields to represent the prior knowledge of fingerprints. Noisy orientation patches outputted by a local estimation approach are replaced by the closest orientation patches in the dictionary. Experimental results on the NIST SD27 latent fingerprint database showed that this approach performs much better than two regularization approaches which are based on smoothing and global surface fitting, respectively. However, a limitation of this method is that the spatial distribution of orientation patches is not taken into account. Due to this limitation, it cannot correct real word errors, i.e., the orientation patch is real but its presence at that location is impossible. Such an error is shown in Fig. 1(c).

2.1.5 Motivation of the Proposed Approach

The proposed approach belongs to the family of dictionary based regularization. The difference from the approach in [7] is that, instead of a single dictionary, a set of localized dictionaries are used here. The use of localized dictionaries is motivated by the fact that ridge orientations in different regions of fingerprints have different characteristics. As illustrated in Fig. 4, while ridge orientations in the central region of fingerprints are very diverse depending on fingerprint pattern types, ridge orientations in the peripheral region lack variety. In addition, the orientation patches in four different peripheral regions are different from each other. Such characteristics of fingerprint orientation fields have its physiological cause according to fingerprint formation theory [39]. Thus, instead of using a single dictionary of orientation patches for the whole fingerprint as [7], we can construct a separate dictionary of orientation patches for each location. Each dictionary contains only orientation patches which are likely to appear at the corresponding location. By using localized dictionaries to correct noisy orientation fields, we hope that both the non-word errors in Fig. 1(b) and the real word errors in Fig. 1(c) can be reduced.

2.2 Fingerprint Pose Estimation

The pose of a fingerprint in an image is given by the fingerprint center (x, y) and the fingerprint direction θ. Figure 5 illustrates the definition of the pose of fingerprint using a photograph of a finger and a fingerprint image. Compared to orientation field estimation, pose estimation is a relatively under-researched topic. Even the ANSI/NIST-ITL

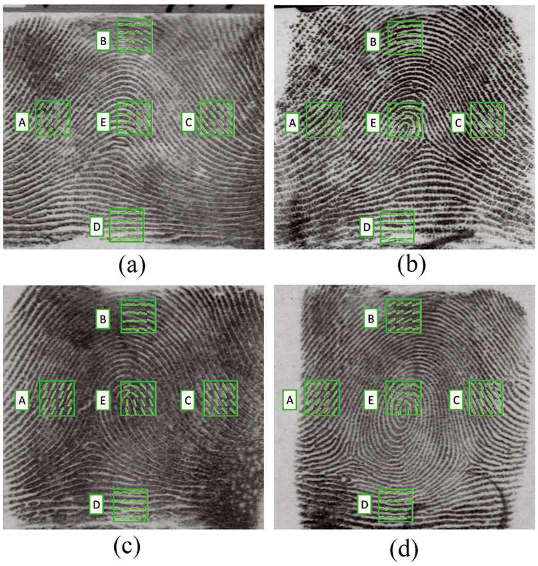

Fig. 4. Ridge orientations in different regions of fingerprints have different characteristics as we can see in these four fingerprints of different pattern types. Ridge orientations in the central region (patch E) of fingerprints are very diverse, while the ones in the peripheral region (patches A, B, C, and D) lack variety and are independent of fingerprint pattern types. In addition, the orientation patches in the four different peripheral regions are different from each other: (a) Arch. (b) Left loop. (c) Right loop. (d) Whorl.

1-2011 standard [40], an significant update over the previous standard, does not provide a clear definition on the center of fingerprints. In this subsection, we first review several approaches which are related to pose estimation and then describe the motivation of the proposed approach.

2.2.1 Region Mask Based Approach

Pose estimation is relatively simple in the case of rolled fingerprints and slap fingerprints. When a rolled fingerprint is complete and has good quality, the barycenter of the foreground region can be used as the fingerprint center [41] and the direction of the left and right boundaries can be used as the fingerprint direction [42]. For slap fingerprints [43], a similar approach can be used. However, this type of approach cannot deal with fingerprints which are of poor quality, incomplete, or have irregular shape. Unfortunately, these situations are common in latent fingerprints.

2.2.2 Distinctive Point Based Approach

Many fingerprint indexing or classification approaches rely on fingerprint registration for fast similarity computation [42], [44]–[46]. But the requirement of fingerprint indexing for registration is different from that of our problem, i.e., statistical modeling of fingerprint orientation fields. The requirement of fingerprint indexing is that different impressions of the same finger can be aligned well, while the requirement of statistical modeling is that all fingerprints can be aligned well. Thus, popular fingerprint registration approaches based on some distinctive point (northernmost loop singularity [14], [47], maximum curvature point [15] or point whose neighboring orientation field meets some properties [42], [48]) do not meet our requirement. In addition, distinctive point detection approaches cannot properly work when the distinctive region is very noisy or not available, which is very common in latent fingerprints (see Fig. 2).

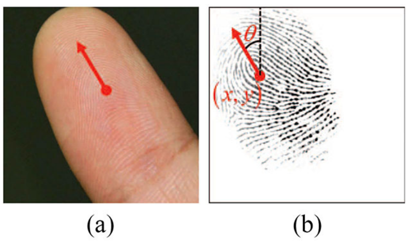

Fig. 5. Definition of the pose (x, y, θ) of fingerprint. (a) Photograph of a fingerprint. (b) Plain impression of a fingerprint.

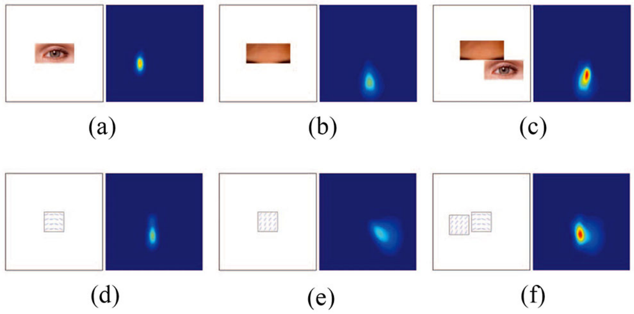

Fig. 6. Predicting the center of a face based on a face part is analogous to predicting the center of a finger based on an orientation patch. In each subfigure, a part is shown on the left and an illustrative probability distribution of the face/finger center is shown on the right. Note that the size of the part is magnified for visualization purpose. (a) Eye. (b) Partial forehead. (c) Combination of an eye and a partial forehead. (d) Distinctive orientation patch. (e) Plain orientation patch. (f) Combination of a distinctive orientation patch and a plain orientation patch.

2.2.3 Focal Point Based Approach

The location of focal point is defined as the crossing point of straight lines normal to ridges [49], [50]. Since these lines usually do not cross at a single point, the average position [49] or barycenter [50] is used. Since multiple curvature centers might be detected, a separate evaluation step is used to choose the optimal one [51]. Similar to the distinctive point based approach, focal point based approach cannot perform properly when the corresponding area is not available or very noisy.

2.2.4 Motivation of the Proposed Approach

To illustrate the idea of the proposed pose estimation algorithm, we make a comparison between finger pose estimation and face pose estimation (see Fig. 6). Here we assume that the directions of both face and finger are frontal and upright and only the centers need to be predicted. Given a small face patch, human can roughly predict the face center. When the patch is distinctive, such as eye, the predicted center is concentrative; While when the patch is not that distinctive, such as a partial forehead, the predicted center is scattered. Similarly, the predicted finger center is concentrative for distinctive orientation patches and scattered for ordinary orientation patches. But, if both patches are given, the prediction will be more concentrative than any single patch.

To incorporate the above idea into an algorithm, we can learn the relative distributions of various orientation patches with respect to finger center in off-line training stage. Given an novel orientation field, we can make prediction based on each orientation patch, accumulate all the predictions and finally detect the peak as the most possible pose.

Such an approach is a type of Hough transform. Hough transform is a general method which has been successfully used to solve a number of computer vision problems, including line detection [52], arbitrary shape detection [53], instance detection [54], object detection [55]–[58], and action recognition [59]. Different from those algorithms, the object here is fingerprint and the voting elements are orientation patches.

3 Pose Estimation

Given a fingerprint image as input, the pose estimation algorithm outputs the pose (x, y, θ) of the finger, which can be used to register the fingerprint into a universal coordinate system (called finger coordinate system and defined by the finger center and direction). Instead of directly using the grayscale image, we infer the fingerprint pose based on the orientation field estimated by a local estimation approach [23], which might be very noisy.

The inference is conducted under a Hough transform framework. Fingerprint orientation fields in different regions have rather different patterns, as Fig. 4 shows. This fact implies that given the pose of a fingerprint and an orientation patch, the location of the patch can be roughly estimated. Conversely, given an orientation patch and its location, the pose of the fingerprint can be roughly estimated. Accumulating the estimation conditioned on different patches will obtain a much concentrative result, as Fig. 6 shows, which indicates a good estimation of the fingerprint pose. To represent the relationship between orientation patch and the pose, we first construct a statistical model $\{\Psi, P_\Psi\}$, $\{\Psi, P_\Psi\}$, where $\Psi = \{\Psi_i\}$ is a set of prototype orientation patches, which compactly represent all the real orientation patches, and P_Ψ is the set of spatial probability distributions of all prototype patches in the finger coordinate system.

In the remaining part of this section, we first present the construction of training orientation fields, then describe how to obtain the prototype orientation patches and how to learn their spatial distributions, and finally present the probabilistic voting algorithm for pose estimation.

3.1 Training Orientation Fields

To generate a reliable statistical model of fingerprint orientation fields, a set of high quality training samples covering major fingerprint pattern types should be prepared first. To achieve this goal, we create a training set by manually marking the orientation fields and the pose of many fingerprints in a public domain database.

The definition of finger center and direction is already shown in Fig. 5. Given a fingerprint image, the direction perpendicular to the finger joint or the ridges located at the bottom area of the fingerprint is chosen as the finger direction. Then the finger center is defined as follows:

- For arch fingerprints, the midpoint of the maximum curvature point and the northernmost straight ridge perpendicular to the finger direction is defined as the center.
- For fingerprints containing one loop and one delta (i.e. tented arch, left loop and right loop), the center is defined as the projective point of the midpoint of the loop and delta on the line which is parallel to the finger direction and crosses the loop.
- For whorl fingerprints, the midpoint of the two loops is defined as the center.

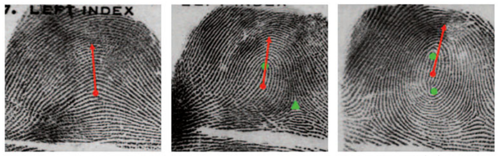

(a) (b) (c)

Fig. 7. Examples of manually marked pose for three types of fingerprints. The red arrow represents the center and direction of fingerprint, the green disk, and triangle represent loop and delta points: (a) Arch. (b) Loop. (c) Whorl.

Fig. 7 shows the manually marked poses of three fingerprints.

The training orientation fields are generated by N_f (398 in our study) real fingerprints from the NIST SD4 rolled fingerprint database. They are registered into a unified coordinate system by manually marking the pose for each of them. Then their blockwise orientation fields are manually marked as the ground truth with the block of 16×16 pixels. These data (including pose and orientation field) are available on the web site (http://ivg.au.tsinghua.edu.cn/).

The training orientation patches are composed of all the $N_\mathrm{p} \times N_\mathrm{p}$ orientation patches of training fingerprints and their locations in the unified coordinate system. Concretely, for each registered training fingerprint, an $N_\mathrm{p} \times N_\mathrm{p}$ window slides from top to bottom, left to right. If all the orientations in a patch are valid, the patch and its center coordinate are recorded. The size of the patch $N_\mathrm{p} \times N_\mathrm{p}$ has a direct impact on representativeness. If patches are too small, the number of prototype patches can be low and their distributions are not informative; If patches are too large, the number of prototype patches will be so high that there are no sufficient samples for estimating the spatial distribution of each prototype patch. Here N_p is empirically set as 4.

3.2 Prototype Orientation Patches

To ensure that the prototype orientation patches are real orientation patches, the well known k-medoids clustering method [60] is employed to pick out a set of representative ones $\{\Psi_i, i = 1, 2, \ldots, k\}$ from all the training orientation patches.

Given the training patches and a predefined k (200 in our study), the k-medoids clustering method consists of three steps: random initialization, assignment, and medoid update. The last two steps are iteratively performed until there is no change in the medoids (namely, the prototype patches). The standard method is used for the last two steps. To ensure diversity of the clustering result, we use a modified random initialization method:

1) The first prototype patch Ψ_1 is randomly selected from all the training patches.

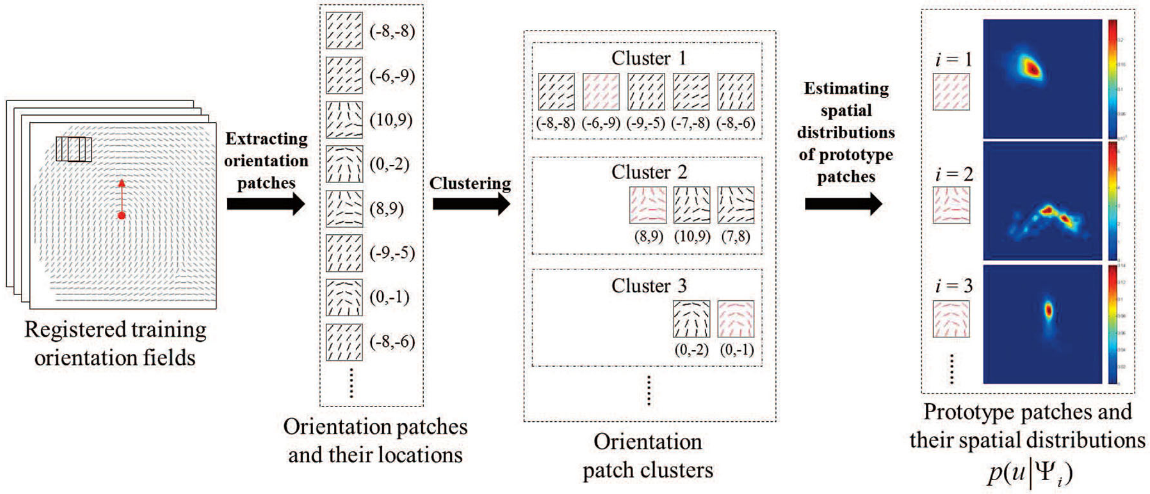

Fig. 8. Flowchart of learning a set of prototype orientation patches and their spatial distributions.

2) Let m denote the number of existing prototypes. The next candidate $\widehat{\Psi}_{m+1}$ is randomly selected from all the unchecked patches, and then the similarity scores between $\widehat{\Psi}_{m+1}$ and existing prototypes $\{\Psi_i, i = 1, 2, \ldots, m\}$ are computed as

$$S_1(\Psi_i, \Psi_j) = \frac{\sum_{l=1}^{N_p}\sum_{n=1}^{N_p}\left(\cos\left(\Psi_i(l,n) - \Psi_j(l,n)\right)\right)^2}{N_p \times N_p} \quad (1)$$

where $\Psi_i(l, n)$ is the orientation element at location (l, n) in patch Ψ_i. If any similarity score is larger than a pre-defined threshold η_1 (empirically set as 0.85), $\widehat{\Psi}_{m+1}$ is discarded and a new candidate is randomly selected and the former diversity examination is performed again. The examination will continue until a $\widehat{\Psi}_{m+1}$ sufficiently different from the existing prototypes is found and then $\widehat{\Psi}_{m+1}$ is determined as a new prototype.

3) Repeat step 2 until k prototypes are obtained.

3.3 Spatial Distributions of Prototype Orientation Patches

The distributions of prototype patches are estimated in a non-parametric manner. The flowchart of the model learning process is shown in Fig. 8. The probability of prototype patch Ψ_i at location $\boldsymbol{u}$ in the finger coordinate system, $p(\Psi_i|\boldsymbol{u})$, is approximated by the frequency of the patches in cluster i occurring at $\boldsymbol{u}$, i.e.

$$p(\Psi_i|\boldsymbol{u}) = \frac{N_{\boldsymbol{u},i}}{N_f}, \quad (2)$$

where $N_{\boldsymbol{u},i}$ is the number of fingerprint orientation patches at $\boldsymbol{u}$ belonging to cluster i and N_f denotes the number of training fingerprints. The prototype patch probability distributions at four representative locations are shown in Fig. 9. As expected, the distributions at four locations are very different.

The prototype patch probability at a certain position can be viewed as prior distribution, while we care more about the spatial posterior probability distribution $p(\boldsymbol{u}|\Psi_i)$. The posterior probability can be easily estimated by Bayes' theorem

$$p(\boldsymbol{u}|\Psi_i) = \frac{p(\Psi_i|\boldsymbol{u})\,p(\boldsymbol{u})}{\sum_{\boldsymbol{u}'} p(\Psi_i|\boldsymbol{u}')\,p(\boldsymbol{u}')} = \frac{p(\Psi_i|\boldsymbol{u})}{\sum_{\boldsymbol{u}'} p(\Psi_i|\boldsymbol{u}')}, \quad (3)$$

where $\boldsymbol{u}'$ is an arbitrary location in the finger coordinate system and we have $p(\boldsymbol{u}) = p(\boldsymbol{u}')$ in general condition. The posterior probability distributions of three prototype patches are shown at the rightmost column of Fig. 8.

3.4 Pose Estimation

Given an input fingerprint, the initial orientation field is estimated and rotated by various angles. For each rotated version, a finger center is estimated by probabilistic voting. The one with the highest value is chosen as the finger center and the corresponding rotation angle is determined as the finger direction. The flowchart of the pose estimation procedure is shown in Fig. 10 and Fig. 11, and the pseudo code corresponding to Fig. 10 is given in Algorithm 1.

The initial orientation field O is estimated by the local Fourier analysis approach in [23]. To deal with strong noise, at most two strongest orientations are estimated for each 16×16 block. The probability of the finger center at position $\boldsymbol{x}$ (In this paper, we use $\boldsymbol{x}$ to represent finger center (x, y)) is estimated by accumulating the voting, $p(\boldsymbol{x}|\Psi^*, \boldsymbol{v})$, of all the available initial orientation patches in the fingerprint image as follows:

$$A(\boldsymbol{x}) = \sum_{\boldsymbol{v}} p\left(\boldsymbol{x}\,|\,\Psi^*, \boldsymbol{v}\right). \quad (4)$$

Ψ^* is the most similar prototype patch of orientation patch $\boldsymbol{o}$ at location $\boldsymbol{v}$ in O, which is defines as:

$$\Psi^* = \arg\max_{\Psi_i} S_2(\boldsymbol{o}, \Psi_i), i = 1, 2, \ldots, k. \quad (5)$$

The similarity between an initial orientation patch and a prototype patch is given by

$$S_2(\boldsymbol{o}, \Psi_i) = n_s/(N_p \times N_p), \quad (6)$$

where n_s is the number of orientation elements whose differences are less than a predefined threshold (empirically

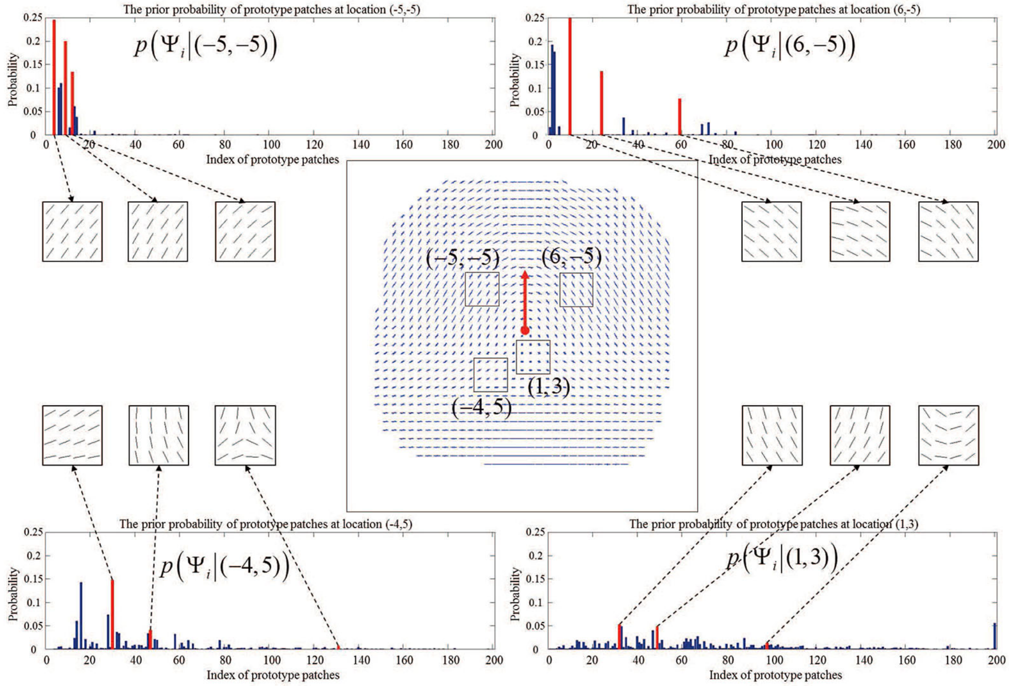

Fig. 9. Orientation field in the middle visualizes the histogram of orientations at each location of a set of registered fingerprints, in which the orientations are grouped into 6 bins and the length of the orientations indicates their frequencies in all training fingerprints. The black frames in the middle image indicate the locations of the patches. The four bar charts show the probabilities of all the prototype orientation patches at four positions.

set as $\pi/18$). Since $\boldsymbol{o}$ may contain two orientation elements in a block, the differences of closer orientation elements are selected.

$p(\boldsymbol{x}|\Psi^*, \boldsymbol{v})$ in equation (4) denotes the probability distribution of finger center $\boldsymbol{x}$ conditioned on Ψ^* at location $\boldsymbol{v}$ and is given by:

$$p(\boldsymbol{x}|\Psi^*, \boldsymbol{v}) = p(\boldsymbol{u}_{\boldsymbol{x}}|\Psi^*), \tag{7}$$

where $\boldsymbol{u}_{\boldsymbol{x}} = \boldsymbol{v} - \boldsymbol{x}$.

To avoid voting by too noisy orientation patches, the patches whose similarity with the most similar prototype patch is lower than a predefined threshold (empirically set as 0.6) do not participate the voting. By accumulating the voting images of all the orientation patches, the Hough image of fingerprint center is obtained. Then the position with maximum value is selected as the center of the fingerprint.

Pose estimation results for six poor quality latents are shown in Fig. 12, where some of the latents have only very small region and the central region is usually not available.

4 Orientation Field Estimation

For most latent fingerprints, the initial orientation fields estimated by the local Fourier analysis approach [23] are often quite noisy and may contain more than one orientations at many locations. We perform orientation

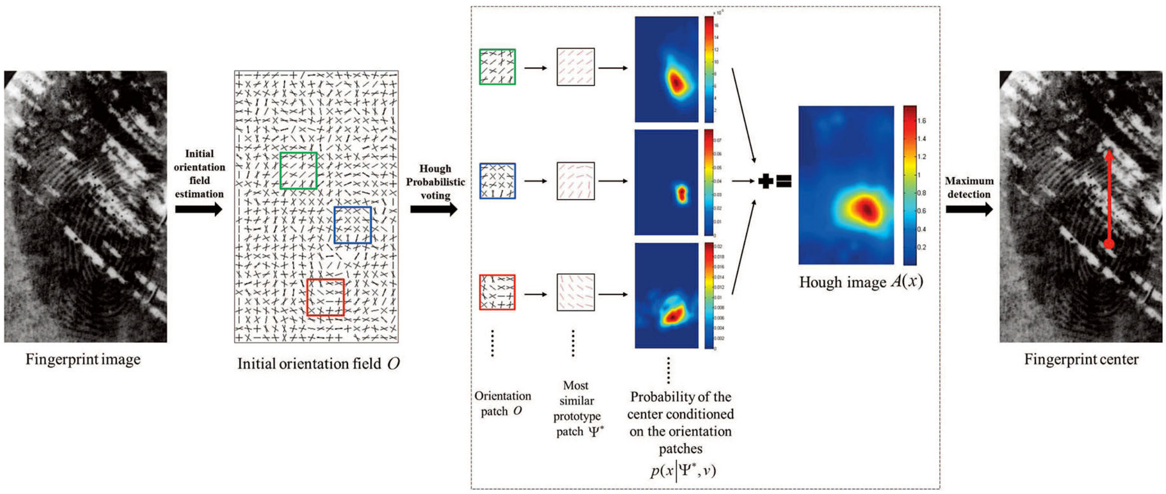

Fig. 10. Flowchart of estimating the finger center of an upright latent fingerprint.

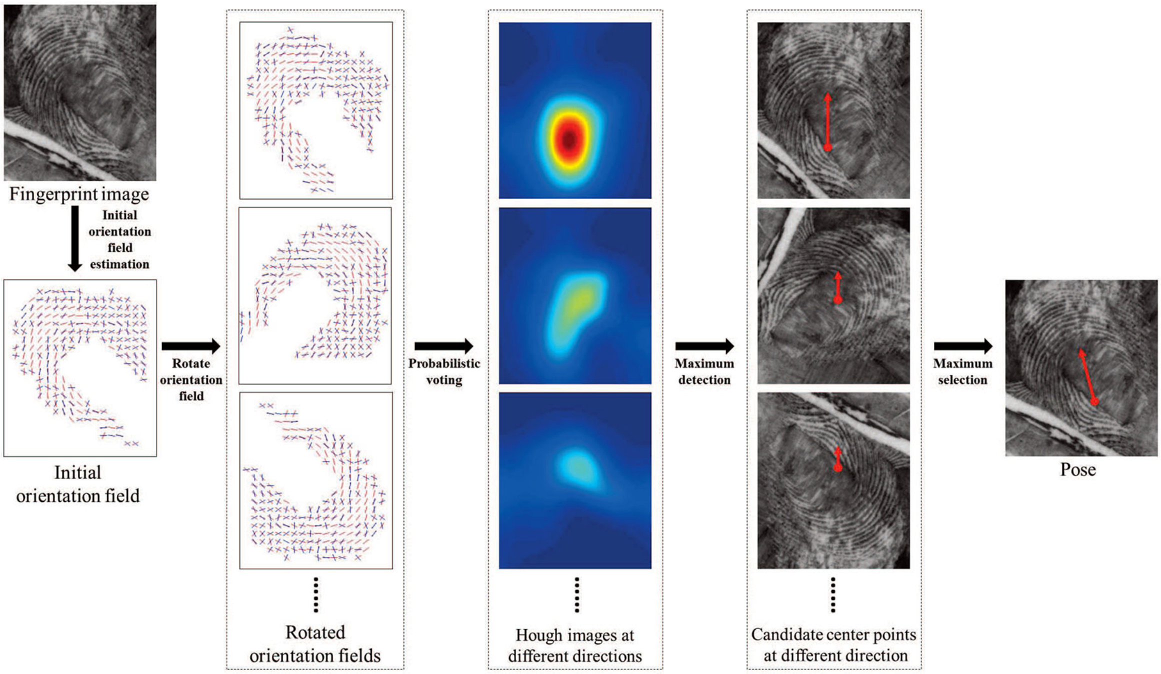

Fig. 11. Pose estimation of a fingerprint with unknown direction. The initial orientation field is rotated by a set of possible angles; the center estimation procedure is then applied to detect the center at each angle; and finally the one with the largest value is chosen.

Algorithm 1 Finger center estimation

Input: Initial orientation field O
  $A = \mathbf{0}$
  for orientation patch at each location v in O **do**
    $\Psi^* \leftarrow$ closest prototype patch
    $A = A + p(x \mid \Psi^*, v)$
  end for
Output: $x^* = \arg\max A$

field regularization to correct errors and determine a single orientation at each location by replacing with similar orientation patches in dictionaries. Since dictionary lookup still cannot resolve ambiguity in difficult cases, we use contextual information through the Markov random field framework [61], [62]. Although the overall approach is similar to [7], the major difference is that we use different dictionaries for different locations instead of a single dictionary.

In the following subsections, we first describe the offline construction of the localized dictionaries and then present the two-step orientation field regularization algorithm which takes the pose calibrated initial orientation field as input and outputs a regularized orientation field. Since the orientation field regularization algorithm based on localized dictionaries closely follows the algorithm in [7], the description is relatively concise here. See [7] for a more complete and detailed description of dictionary based orientation field regularization.

4.1 Constructing Localized Dictionaries

A localized dictionary D_u at location $\boldsymbol{u}$ in the finger coordinate system is obtained by clustering the set T_u of all training patches (here the patch size is empirically set as 6×6) at a small neighborhood around $\boldsymbol{u}$ using the following procedure:

1) The first orientation patch in T_u is added into D_u.
2) The similarities between the next patch in T_u and all the patches in D_u are computed using equation (6). If all the similarities are less than a predefined threshold (empirically set as 0.8), the patch is added into D_u.
3) Repeat step 2 until all the patches in T_u have been checked.

After performing the above clustering procedure for all locations, we obtain a set of localized dictionaries $\{D_u\}$. Since the characteristics of ridge orientations at different locations are rather different, the sizes of localized dictionaries (namely, the number of orientation patches in a localized dictionary) vary according to the location (from less than 10 to around 600, the average size is 95). The size of a localized dictionary at a location is closely

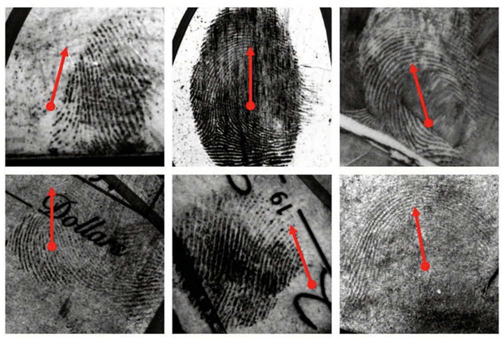

Fig. 12. Proposed pose estimation algorithm is able to correctly estimate the poses of many very incomplete and noisy latent fingerprints.

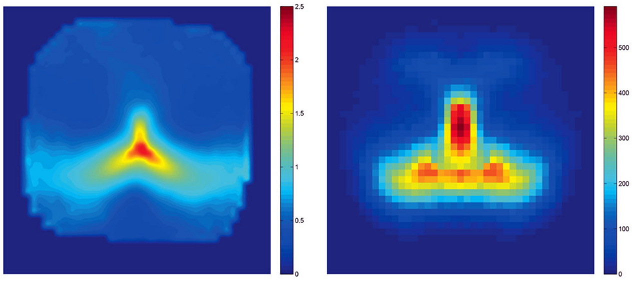

(a) (b)

Fig. 13. Correlation between the variation of orientation and the size (the number of orientation patches) of localized dictionaries. (a) Image of circular standard deviation at each location of registered training orientation fields. (b) Image of size of localized dictionaries. Red color indicates large value while blue color indicates small value. Generally, larger deviation indicates larger dictionary size while smaller deviation indicates smaller dictionary size.

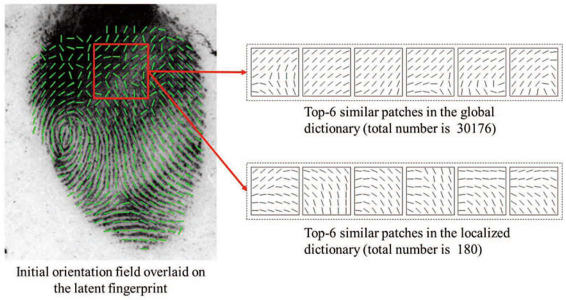

Fig. 14. Different lookup results of global dictionary and localized dictionary for a noisy initial orientation patch (marked by the red box). Because the initial orientation patch is very noisy, none of the top six similar patches in the global dictionary is close the true ridge orientations. But the top six similar patches in the localized dictionary contain several good estimates.

correlated with the circular standard deviation of local ridge orientation at the same location, as shown in Fig. 13.

4.2 Dictionary Lookup

Using the pose estimated by the pose estimation algorithm described in section 3, the initial orientation field is registered into the finger coordinate system with the finger center being the origin and the finger direction being y-axis. Then the registered orientation field is regularized by localized dictionaries lookup and context-based correction.

The diagram of localized dictionaries lookup is illustrated in Fig. 3. Firstly, the registered orientation field is partitioned into a set of overlapping orientation patches. Then, at each location $\boldsymbol{u}$, the top-N_c (empirically set as 6) candidate patches in the localized dictionary $D_{\boldsymbol{u}}$ which are most similar to the initial orientation patch $\boldsymbol{o}$ are selected with diversity examination. Refer to [7] for more details of this step.

Dictionary lookup using localized dictionaries has two advantages over using a global dictionary: 1) patches which are not likely to appear in a specific position are avoided and 2) the number of the patches in a localized dictionary is much smaller than the global one. The average size of a localized dictionary is 95, while the global dictionary has about 30K patches. As we can see from the example in Fig. 14, due to the severe noise, none of the top six candidates found in the global dictionary is similar to the true orientation patch, while the correct orientation patch can be retrieved within the top six candidates by using the localized dictionary.

4.3 Context-Based Orientation Field Correction

After dictionary lookup, N_c candidate patches are generated for each initial patch. Then context-based orientation field correction algorithm is used to select the most proper candidate considering local similarity and neighborhood compatibility simultaneously. The procedure is the same as the one in [7], i.e. minimizing an energy function:

$$E(\mathbf{r}) = E_s(\mathbf{r}) + \omega_c E_c(\mathbf{r}), \tag{8}$$

where $\mathbf{r}$ denotes the indices of determined candidate patches, $E_s(\mathbf{r})$ denotes the similarity term, $E_c(\mathbf{r})$ denotes the compatibility term, and ω_c is the weight. The energy function is minimized using the loopy belief propagation algorithm [61]. Refer to [7] for more details of this step.

5 Experimental Results

In this section, we first introduce the databases for performance evaluation in our work. Then the matching performances of our algorithm and several representative algorithms on these databases are reported and compared.

5.1 Databases

To evaluate the performance of our method, three latent fingerprint databases are used, including the NIST SD27 latent fingerprint database, Hisign latent fingerprint database, and Tsinghua Overlapped Latent Fingerprint (OLF) database. The proposed method is also tested on the fingerprint orientation extraction (FOE) benchmark of FVC-onGoing [17], [63], [64], which contains low quality fingerprints captured using optical scanners.

NIST SD27 is the most widely used public domain latent fingerprint database, which is composed of 258 latent fingerprints and corresponding rolled ones. Most latents in NIST SD27 are of very poor quality, with unclear ridge structures, complex background and overlapping patterns. Hisign latent fingerprint database contains 673 latent fingerprints (three examples are shown in Fig. 15(a)) and corresponding rolled ones. All latents in this database are from solved cases and the average image quality is better than NIST SD27. Tsinghua Overlapped Latent Fingerprint database contains 100 overlapped latent fingerprints developed using magnetic powder and corresponding plain fingerprints. The FOE-STD-1.0 benchmark in FVC-onGoing is an on-line automated evaluation system for fingerprint orientation extraction, which includes 10 fingerprints of good quality and 50 fingerprints of low quality. Note that the fingerprints in the FOE benchmark are not accessible to the participants.

In addition, 27,000 rolled fingerprints (file fingerprints) in NIST SD14 were used as the background database in the latent matching experiments to make the evaluation more

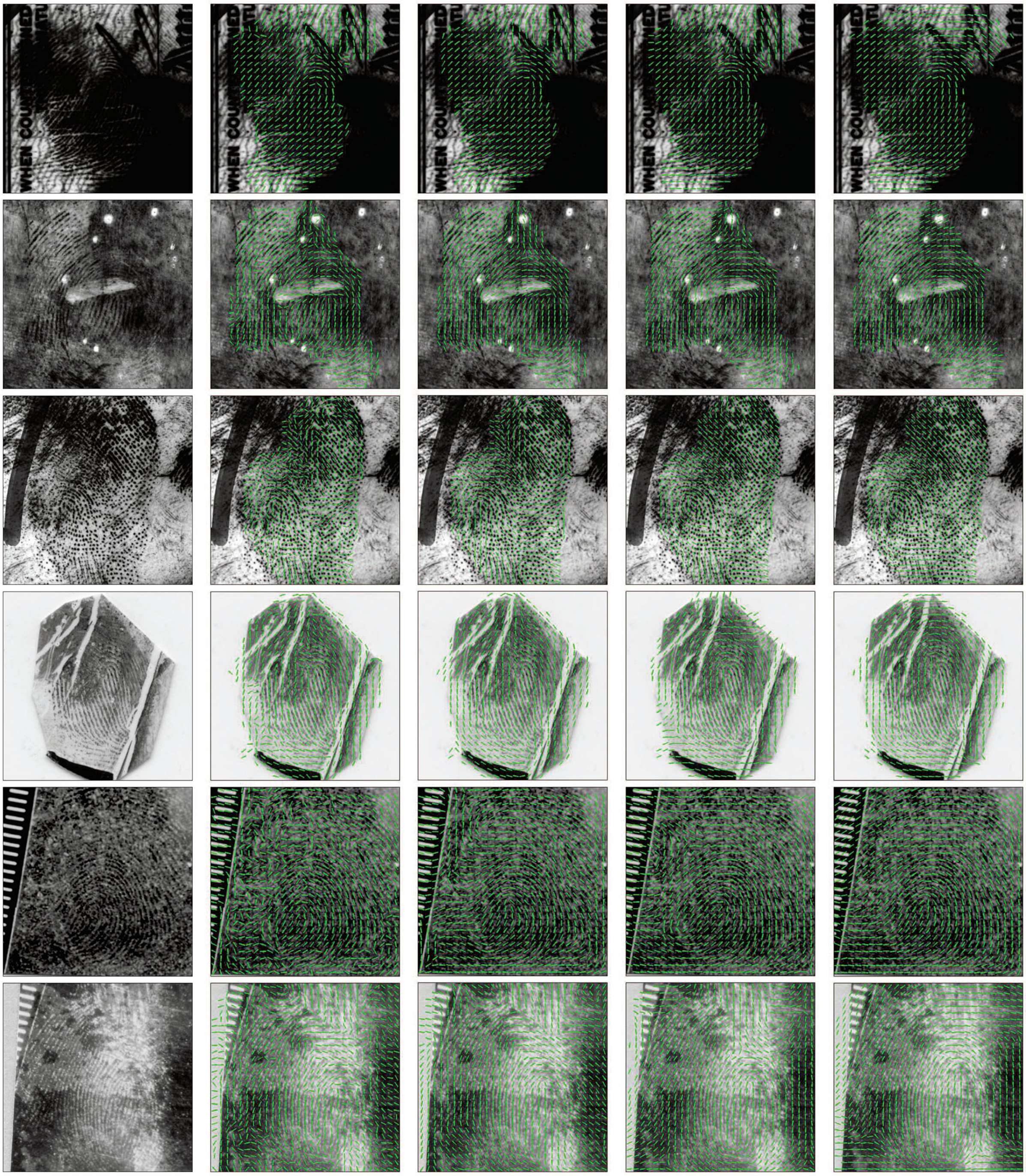

(a) (b) (c) (d) (e)

Fig. 15. Comparison of orientation fields estimated by four algorithms (STFT, FOMFE, GlobalDict, and the proposed). The top three latent fingerprints are from the NIST SD27 latent database, while the bottom three are from the Hisign latent database.

realistic and challenging. Table 1 provides a summary of the databases used in this work.

5.2 Performance

Three types of evaluations were performed:

1) direct evaluation of the accuracy of orientation field estimation on the NIST SD27 latent database and the FVC-onGoing FOE benchmark,
2) evaluation of matching accuracy on the NIST SD27 and Hisign latent databases, and
3) evaluation of separating overlapped latent fingerprints on the Tsinghua Overlapped Latent Fingerprint database.

For the evaluations on the NIST SD27 database, besides the proposed algorithm, three additional algorithms are included:

1) combination of gradient-based local estimation and FOMFE-based global model [31],
2) combination of STFT-based local estimation and low pass filtering [6], and

TABLE 1
Fingerprint Databases Used in This Study

Database	Description	Purpose
NIST SD4	2,000 pairs of rolled fingerprints; http://www.nist.gov/srd/nistsd4.cfm	statistical model learning, dictionary construction
NIST SD14	27,000 pairs of rolled fingerprints; http://www.nist.gov/srd/nistsd14.cfm	background database
NIST SD27	258 pairs of latent fingerprints and mated rolled fingerprints; http://www.nist.gov/srd/nistsd27.cfm	algorithm evaluation
Tsinghua Overlapped Latent	100 overlapped latent fingerprints and 12 mated plain fingerprints; http://ivg.au.tsinghua.edu.cn	algorithm evaluation
Hisign latent	673 pairs of latent fingerprints and mated rolled fingerprints	algorithm evaluation
FOE-STD-1.0 on FVC-onGoing	10 fingerprints of good quality and 50 fingerprints of bad quality	algorithm evaluation

3) dictionary lookup based on a global dictionary (referred to as GlobalDict hereinafter) [7].

For overlap separating evaluation, besides the proposed algorithm and GlobalDict, a special-purpose separating algorithm [65] is included.

5.2.1 Accuracy of Orientation Field Estimation

The purpose of introducing localized dictionaries is to reduce both non-word errors and real word errors in estimating orientation field. As shown in the six examples in Fig. 15, the proposed algorithm does produce much fewer errors than the rest three orientation field estimation algorithms. Note that for the latents in the NIST SD27 database, which contain structured noise or even multiple fingerprints, manually marked region masks are used as previous work [7], [37], [38], while for the latents in the Hisign database, region masks are automatically estimated by comparing the magnitude of strongest waves to a threshold.

The accuracy of orientation field estimation algorithms is quantitatively measured by the average Root Mean Square Deviation (RMSD) of the estimated orientation fields from the ground truth orientation fields, as suggested in [17]. The ground truth orientation fields of the NIST SD27 latent database have been manually marked by one of the authors. Average RMSDs of the four algorithms (STFT, FOMFE, GlobalDict, and the proposed) are computed both for the overall NIST SD27 database and three subsets belonging to three quality levels (Good, Bad and Ugly). To evaluate the impact of pose estimation on orientation field estimation, we replace the automatically estimated pose by manually marked pose and test the proposed algorithm too. To ensure that the manually marked pose is optimal, the mated rolled fingerprint is also displayed when marking the pose of latent. As shown in Table 2, the proposed algorithm consistently outperforms the rest three algorithms, while the utilization of manually marked pose obtains a slightly better result. The improvement brought by manually marked pose is not significant due to two reasons.

TABLE 2
Average Estimation Error (in Degrees) of the Proposed and Three Published Orientation Estimation Algorithms on the NIST SD27 Database

Algorithm	All	Good	Bad	Ugly
Proposed (manually marked pose)	13.76	10.87	14.12	16.40
Proposed	14.35	11.15	15.15	16.85
GlobalDict [7]	18.44	14.40	19.18	21.88
FOMFE [31]	28.12	22.83	29.09	32.63
STFT [6]	32.51	27.27	34.10	36.36

Firstly, an incorrectly estimated pose for incomplete fingerprints does not necessarily produce incorrect orientation fields (see the example in Fig. 16). Secondly, for very poor quality latents, the current algorithm does not benefit much from the given pose.

The proposed algorithm has been submitted to the FVC-onGoing FOE benchmark and the result has been published on the web site [64]. Its average error on the bad quality dataset is 9.66 degrees and ranks first, indicating that it can be applied to low quality livescan fingerprints as well.

5.2.2 Matching Accuracy

Our final goal of estimating orientation field is to improve latent matching accuracy. Thus, different orientation field estimation algorithms are further compared by conducting matching experiment on the NIST SD27 and Hisign latent databases (using NIST SD14 as the background database). For each fingerprint (both latent and rolled fingerprints), an orientation field is estimated using each orientation field

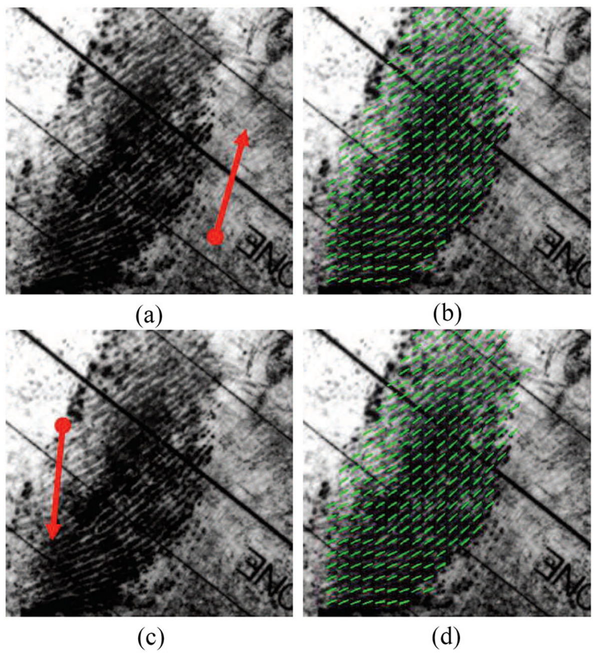

Fig. 16. Wrong estimate of pose does not necessarily impact the estimation of orientation field. (a) True pose. (b) Orientation field estimated based on the true pose. (c) Incorrectly estimated pose. (d) Orientation field estimated based on the incorrect pose.

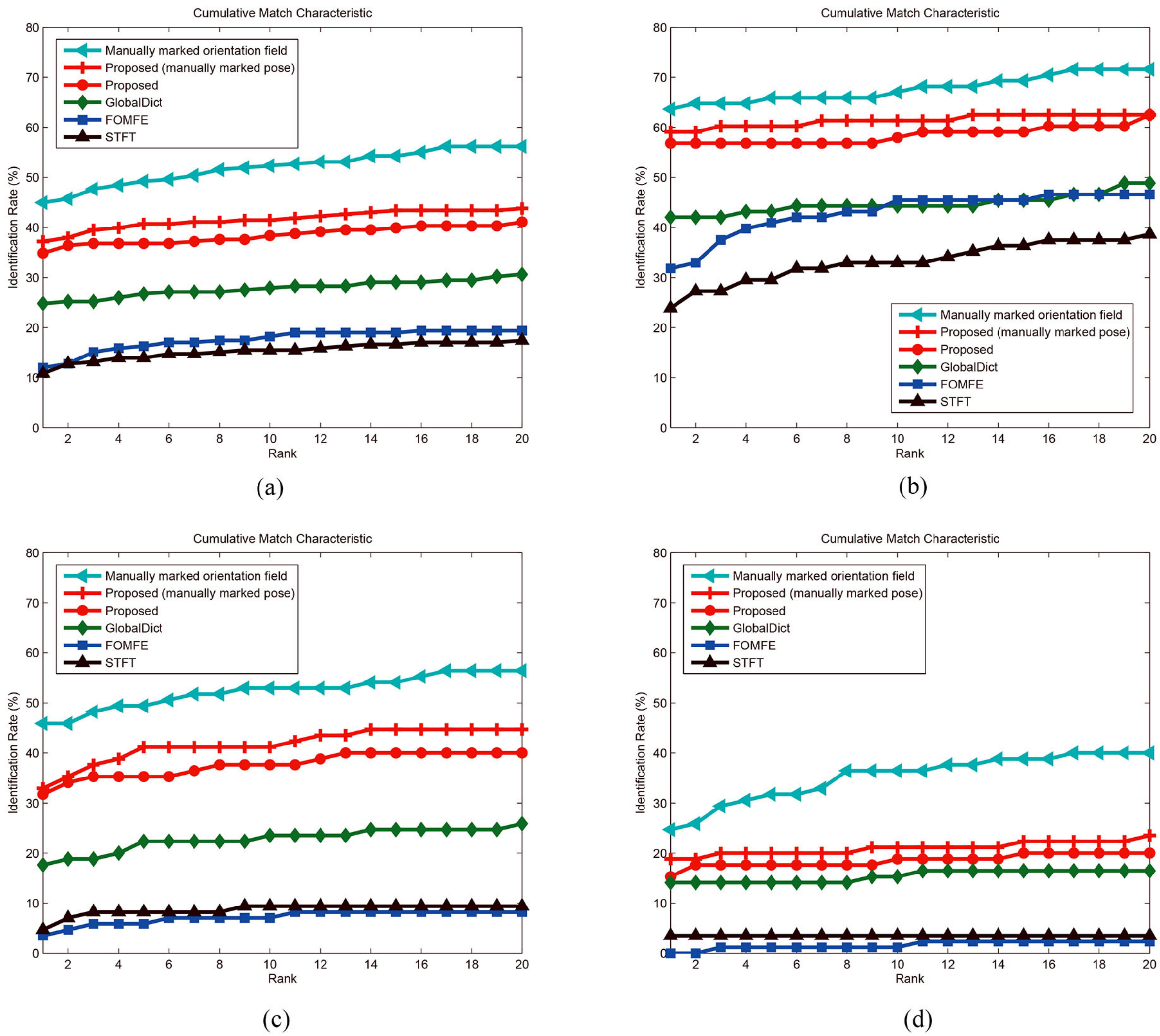

Fig. 17. CMC curves of six orientation field estimation approaches (manual marking, the proposed algorithm with manually marked pose, the proposed algorithm with automatically estimated pose, GlobalDict, FOMFE, and STFT) on the NIST SD27 latent database and subsets: (a) all (258 latents); (b) good quality (88 latents); (c) bad quality (85 latents); and (d) ugly quality (85 latents).

algorithm. To make the comparison fair, the same fingerprint enhancement approach [10] is combined with different orientation field estimation algorithms. The parameters of the Gabor filter are set as follows: the local ridge frequency is fixed at 1/9 cycles per pixel, the standard deviations of the Gaussian envelope are fixed as 4, and the local ridge orientation is tuned to the estimated orientation field. VeriFinger SDK 6.2 [66] is used to extract minutiae from enhanced fingerprints (both latent and rolled fingerprints). The same SDK is then used to compute the match scores between latents and rolled fingerprints. Finally, the Cumulative Match Characteristic (CMC) curve is used to evaluate the matching performance. Although VeriFinger is not designed to encode and match latent fingerprints, it is arguably the best commercial fingerprint SDK which is available to the research community, with high full fingerprint matching accuracy and fast matching speed. It can serve our goal of measuring the relative performances of different fingerprint orientation field estimation algorithms. It also allows fair comparison between algorithms from different research groups since it has been widely used by other researchers.

The CMC curves on the NIST SD27 latent database and the three subsets are shown in Fig. 17 for six different orientation field estimation approaches (manual marking, the proposed algorithm with manually marked pose, the proposed algorithm with automatically estimated pose, GlobalDict, FOMFE, and STFT). As we can see from these curves, there is a clear gap between the GlobalDict algorithm and the two traditional algorithms (FOMFE and STFT), and there is a clear gap between the proposed algorithm and the GlobalDict algorithm. Note that the result of manually marked orientation field is much better than the one in Fig. 13 in [7]. Since the only difference is that in [7] the rolled fingerprints are directly fed to VeriFinger and here the enhanced (by the proposed approach) rolled fingerprints are fed to VeriFinger, we can conclude that the proposed approach outperforms VeriFinger in the case of rolled fingerprints too.

The CMC curves on the Hisign latent database are shown in Fig. 18. Similarly, there is a clear gap between the GlobalDict algorithm and the two traditional algorithms (FOMFE and STFT), and there is a clear gap between the proposed algorithm and the GlobalDict algorithm. The

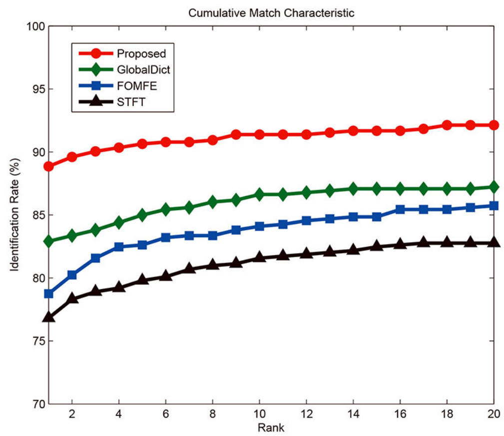

Fig. 18. CMC curves of four orientation field estimation algorithms on the Hisign latent database.

relatively high accuracy on the Hisign latent database is due to that the latents in this database have been cropped by latent examiners to remove background noise and these latents (with manually marked minutiae) were identified by AFIS at high rank on a large database.

5.2.3 Separating Overlapped Latent Fingerprints

In an overlapped latent fingerprint image, the noise is from another fingerprint. This characteristic makes traditional orientation field estimation algorithms totally fail in the case of overlapped latents, since there is an implicit assumption in most orientation field estimation approaches that the noise is randomly distributed. To address the problem, several specific algorithms have been proposed for separating overlapped fingerprints [65], [67], [68]. Given a region mask for the latent fingerprint of interest, the proposed method can be directly apply to these fingerprints (note that the constrained relaxation labeling algorithm [65] and the GlobalDict algorithm [7] require the region masks of both the fingerprint of interest and the overlapping area). The CMC curves on the Tsinghua OLF database in Fig. 19 show that the proposed method even outperforms the specially designed algorithm.

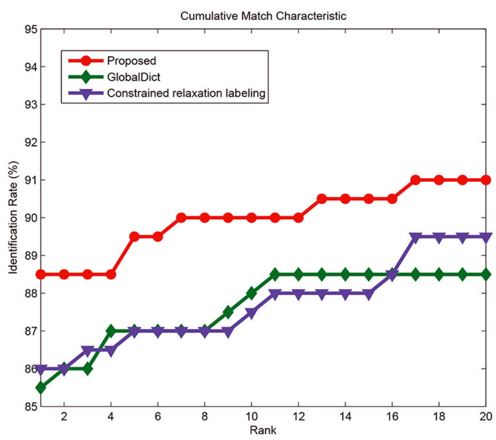

Fig. 19. CMC curves of three orientation field estimation algorithms on the Tsinghua Overlapped Latent Fingerprint database.

TABLE 3
Computation Times (in Seconds) of the Major Steps of the Proposed Algorithm on Different Databases

Step	NIST SD27	Hisign Latent	Tsinghua OLF	NIST SD14
Initial orientation field estimation	3.5	9.6	13.5	22.2
Pose estimation	3.2	5.7	4.4	7.3
Orientation field regularization	0.94	1.8	1.2	2.2
Enhancement	0.95	1.7	1.1	2.1

5.2.4 Computational Complexity

Although the efficiency of automatic latent fingerprint feature extraction is not a critical issue in forensic applications, it is still an important performance measure of an algorithm. The computational costs of the main steps of the proposed approach are tested on a PC with 3.30 GHz CPU. In the off-line training stage, due to large amount of training orientation patches (about 436,000 patches extracted from 398 real fingerprints), the k-medoids clustering based prototype patch and spatial distribution learning takes about 23.6 hours. The construction of localized dictionaries takes about 0.72 hours, while the construction of a global dictionary spends about 7.5 hours. Constructing localized dictionaries are faster because 1) the time complexity of the clustering algorithm is $O(n^2)$, where n is the number of samples, and 2) the construction of each local dictionary uses only orientation patches in the same location. All the off-line training steps are implemented in MATLAB. In the on-line stage, the average times of processing fingerprints from different databases are shown in Table 3. Among the four steps, pose estimation is implemented in C language while the others are implemented in MATLAB.

6 Summary and Future Work

Estimation of fingerprint orientation field is a critical step in automatic fingerprint recognition. A number of algorithms have been published on this topic and the performance of the state-of-the-art algorithms is fairly good for most livescan and inked fingerprints. But in the case of latent fingerprints, the performance of these algorithms is still far from satisfactory. To deal with the severe noise in many latent fingerprints, prior knowledge of fingerprints should be taken into account.

The study in [7] shows that utilization of prior knowledge of fingerprints in orientation field estimation is very promising. But the use of a single global dictionary for the whole fingerprint has a drawback: valid local ridge patterns may appear at an impossible location of fingerprint. This problem is analogous to real word error in spelling correction.

A natural idea to overcome the limitation of global dictionary is to replace it with a set of localized dictionaries. But a big obstacle to localized dictionaries is that the pose of the fingerprint need to be known. Estimating fingerprint pose from poor quality latent fingerprints is a very challenging problem and also a very under-researched topic.

In this paper, we propose a Hough transform based fingerprint pose estimation method and a localized dictionary lookup based fingerprint orientation field estimation method. Based on the spatial distributions of the prototype orientation patches, which are learned from a set of registered training orientation fields, the proposed pose estimation method is robust against the problems of low image quality and small available region. Since the pose of the fingerprint is reliably estimated, the location-dependent prior knowledge of fingerprint orientation fields is able to guide orientation field regularization. The experimental results on two latent fingerprint databases demonstrate the superiority of the proposed algorithm comparing with three representative orientation field estimation algorithms, and the results on the overlapped latent fingerprint database show that the proposed approach performs even better than the specially designed state-of-the-art algorithm. Although targeted for latent fingerprints, this algorithm can deal with low quality plain and rolled fingerprints as shown in the experiments.

However, the proposed algorithm can be still improved in several ways:

1) constructing a framework to optimize the variables in this work, such as the number of training orientation fields, the number of prototype patches, the size of prototype patches, and the size of the patches in the dictionaries and so on;
2) developing hierarchical approaches for pose estimation and orientation field regularization since the current scheme is too time consuming for civilian applications;
3) developing an automatic region segmentation algorithm for latent fingerprints with strong structured noise or overlapping fingerprints.

ACKNOWLEDGMENTS

This work is supported by the National Natural Science Foundation of China under Grants 61005023, 61373074, 61225008 and 61020106004, the National Basic Research Program of China under Grant 2014CB349304, the Ministry of Education of China under Grant 20120002110033, and the Tsinghua University Initiative Scientific Research Program.

REFERENCES

[1] C. Champod, C. Lennard, P. Margot, and M. Stoilovic, *Fingerprints and Other Ridge Skin Impressions*. Boca Raton, FL, USA: CRC Press, 2004.

[2] A. K. Jain and J. Feng, "Latent fingerprint matching," *IEEE Trans. Pattern Anal. Mach. Intell.*, vol. 33, no. 1, pp. 88–100, Jan. 2011.

[3] V. N. Dvornychenko and M. D. Garris, "Summary of NIST latent fingerprint testing workshop," NIST, Gaithersburg, MD, USA, Int. Rep. 7377, 2006.

[4] *The FBI's Next Generation Identification (NGI)* [Online]. Available: http://www.fbi.gov/about-us/cjis/fingerprints$_b$iometrics/ngi

[5] M. Indovina *et al.*, "ELFT Phase II–An evaluation of automated latent fingerprint identification technologies," NIST, Gaithersburg, MD, USA, Int. Rep. 7577, 2009.

[6] S. Chikkerur, A. N. Cartwright, and V. Govindaraju, "Fingerprint enhancement using STFT analysis," *Pattern Recognit.*, vol. 40, no. 1, pp. 198–211, 2007.

[7] J. Feng, J. Zhou, and A. K. Jain, "Orientation field estimation for latent fingerprint enhancement," *IEEE Trans. Pattern Anal. Mach. Intell.*, vol. 35, no. 4, pp. 925–940, Apr. 2013.

[8] L. O'Gorman and J. V. Nickerson, "An approach to fingerprint filter design," *Pattern Recognit.*, vol. 22, no. 1, pp. 29–38, 1989.

[9] B. G. Sherlock, D. M. Monro, and K. Millard, "Fingerprint enhancement by directional Fourier filtering," *IEE Proc. Vision, Image Signal Process.*, vol. 141, no. 2, pp. 87–94, Apr. 1994.

[10] L. Hong, Y. Wan, and A. K. Jain, "Fingerprint image enhancement: Algorithm and performance evaluation," *IEEE Trans. Pattern Anal. Mach. Intell.*, vol. 20, no. 8, pp. 777–789, Aug. 1998.

[11] T. Kamei, "Image filter design for fingerprint enhancement," in *Automatic Fingerprint Recognition Systems*, N. Ratha and R. Bolle, Eds. New York, NY, USA: Springer, 2004, pp. 113–126.

[12] F. Turroni, R. Cappelli, and D. Maltoni, "Fingerprint enhancement using contextual iterative filtering," in *Proc. 5th IAPR ICB*, New Delhi, India, 2012, pp. 152 – 157.

[13] K. Kukich, "Techniques for automatically correcting words in text," *ACM CSURV*, vol. 24, no. 4, pp. 377–439, 1992.

[14] A. M. Bazen and S. H. Gerez, "Systematic methods for the computation of the directional fields and singular points of fingerprints," *IEEE Trans. Pattern Anal. Mach. Intell.*, vol. 24, no. 7, pp. 905–919, Jul. 2002.

[15] M. Liu, X. Jiang, and A. C. Kot, "Fingerprint reference-point detection," *EURASIP J. Appl. Signal Process.*, vol. 2005, no. 4, pp. 498–509, 2005.

[16] D. Maltoni, D. Maio, A. K. Jain, and S. Prabhakar, *Handbook of Fingerprint Recognition*, 2nd ed. New York, NY, USA: Springer, 2009.

[17] F. Turroni, D. Maltoni, R. Cappelli, and D. Maio, "Improving fingerprint orientation extraction," *IEEE Trans. Inf. Forensics Security*, vol. 6, no. 3, pp. 1002–1013, Sep. 2011.

[18] M. Kass and A. Witkin, "Analyzing oriented patterns," *CVGIP*, vol. 37, no. 3, pp. 362–385, 1987.

[19] N. K. Ratha, S. Chen, and A. K. Jain, "Adaptive flow orientation-based feature extraction in fingerprint images," *Pattern Recognit.*, vol. 28, no. 11, pp. 1657–1672, 1995.

[20] J. Bigun and G. H. Granlund, "Optimal orientation detection of linear symmetry," in *Proc. 1st ICCV*, London, U.K., 1987, pp. 433–438.

[21] B. Mehtre, N. Murthy, S. Kapoor, and B. Chatterjee, "Segmentation of fingerprint images using the directional image," *Pattern Recognit.*, vol. 20, no. 4, pp. 429–435, 1987.

[22] M. A. Oliveira and N. J. Leite, "A multiscale directional operator and morphological tools for reconnecting broken ridges in fingerprint images," *Pattern Recognit.*, vol. 41, no. 1, pp. 367–377, 2008.

[23] A. K. Jain and J. Feng, "Latent palmprint matching," *IEEE Trans. Pattern Anal. Mach. Intell.*, vol. 31, no. 6, pp. 1032–1047, Jun. 2009.

[24] Method and apparatus for adaptive hierarchical processing of print images, by P. Z. Lo and Y. Lo. (2007). *U.S. Patent 11/456 622* [Online]. Available: http://www.google.com/patents/US20070292005

[25] S. C. Dass, "Markov random field models for directional field and singularity extraction in fingerprint images," *IEEE Trans. Image Process.*, vol. 13, no. 10, pp. 1358–1367, Oct. 2004.

[26] K. C. Lee and S. Prabhakar, "Probabilistic orientation field estimation for fingerprint enhancement and verification," in *Proc. BSYM*, Tampa, FL, USA, 2008, pp. 41–46.

[27] Z. Hou, H.-K. Lam, W.-Y. Yau, and Y. Wang, "A variational formulation for fingerprint orientation modeling," *Pattern Recognit.*, vol. 45, no. 5, pp. 1915–1926, 2012.

[28] J. Gu, J. Zhou, and C. Yang, "Fingerprint recognition by combining global structure and local cues," *IEEE Trans. Image Process.*, vol. 15, no. 7, pp. 1952–1964, Jul. 2006.

[29] S. Ram, H. Bischof, and J. Birchbauer, "Modelling fingerprint ridge orientation using Legendre polynomials," *Pattern Recognit.*, vol. 43, no. 1, pp. 342–357, 2010.

[30] S. Jirachaweng, Z. Hou, W.-Y. Yau, and V. Areekul, "Residual orientation modeling for fingerprint enhancement and singular point detection," *Pattern Recognit.*, vol. 44, no. 2, pp. 431–442, 2011.

[31] Y. Wang, J. Hu, and D. Phillips, "A fingerprint orientation model based on 2D Fourier expansion (FOMFE) and its application to singular-point detection and fingerprint indexing," *IEEE Trans. Pattern Anal. Mach. Intell.*, vol. 29, no. 4, pp. 573–585, Apr. 2007.

[32] B. G. Sherlock and D. M. Monro, "A model for interpreting fingerprint topology," *Pattern Recognit.*, vol. 26, no. 7, pp. 1047–1055, 1993.

[33] J. Zhou and J. Gu, "A model-based method for the computation of fingerprint's orientation field," *IEEE Trans. Image Process.*, vol. 13, no. 6, pp. 821–835, Jun. 2004.

[34] J. Gu, J. Zhou, and D. Zhang, "A combination model for orientation field of fingerprints," *Pattern Recognit.*, vol. 37, no. 3, pp. 543–553, 2004.
[35] J. Li, W.-Y. Yau, and H. Wang, "Constrained nonlinear models of fingerprint orientations with prediction," *Pattern Recognit.*, vol. 39, no. 1, pp. 102–114, 2006.
[36] S. Huckemann, T. Hotz, and A. Munk, "Global models for the orientation field of fingerprints: An approach based on quadratic differentials," *IEEE Trans. Pattern Anal. Mach. Intell.*, vol. 30, no. 9, pp. 1507–1519, Sep. 2008.
[37] S. Yoon, J. Feng, and A. K. Jain, "On latent fingerprint enhancement," in *Proc. SPIE* , 2010.
[38] S. Yoon, J. Feng, and A. K. Jain, "Latent fingerprint enhancement via robust orientation field estimation," in *Proc. IJCB*, Washington, DC, USA, 2011, pp. 1–8.
[39] M. Kücken and A. C. Newell, "Fingerprint formation," *J Theor. Biol.*, vol. 235, no. 1, pp. 71–83, 2005.
[40] *ANSI/NIST-ITL 1-2011 Standard* [Online]. Available: http://biometrics.nist.gov/cs_links/standard/AN_ANSI_1-2011_standard.pdf
[41] R. Cappelli and D. Maltoni, "On the spatial distribution of fingerprint singularities," *IEEE Trans. Pattern Anal. Mach. Intell.*, vol. 31, no. 4, pp. 742–448, Apr. 2009.
[42] G. T. Candela, P. J. Grother, C. I. Watson, R. A. Wilkinson, and C. L. Wilson, "PCASYS-A: Pattern-Level classification automation system for fingerprints," NIST, Gaithersburg, MD, USA, Int. Rep. 5647, 1995.
[43] C. Watson, P. Flanagan, and B. Cochran, "SlapSegII: Slap fingerprint segmentation evaluation II," NIST, Gaithersburg, MD, USA, Int. Rep. 7553, 2009.
[44] A. K. Jain, S. Prabhakar, and L. Hong, "A multichannel approach to fingerprint classification," *IEEE Trans. Pattern Anal. Mach. Intell.*, vol. 21, no. 4, pp. 348–359, Apr. 1999.
[45] M. Liu, X. Jiang, and A. C. Kot, "Efficient fingerprint search based on database clustering," *Pattern Recognit.*, vol. 40, no. 6, pp. 1793–1803, 2007.
[46] R. Cappelli, "Fast and accurate fingerprint indexing based on ridge orientation and frequency," *IEEE Trans. Syst., Man, Cybern. B, Cybern.*, vol. 41, no. 6, pp. 1511–1521, Dec. 2011.
[47] K. Nilsson and J. Bigun, "Localization of corresponding points in fingerprints by complex filtering," *Pattern Recognit. Lett.*, vol. 24, no. 13, pp. 2135–2144, 2003.
[48] A. K. Jain, S. Prabhakar, L. Hong, and S. Pankanti, "Filterbank-based fingerprint matching," *IEEE Trans. Image Process.*, vol. 9, no. 5, pp. 846–859, May 2000.
[49] S. Novikov and V. S. Kot, "Singular feature detection and classification of fingerprints using Hough transform," in *Proc. 6th SPIE*, vol. 3346. 1998, pp. 259–269.
[50] K. Rerkrai and V. Areekul, "A new reference point for fingerprint recognition," in *Proc. ICIP*, vol. 2. Vancouver, BC, Canada, 2000, pp. 499 – 502.
[51] V. Areekul, K. Suppasriwasuseth, and S. Jirachawang, "The new focal point localization algorithm for fingerprint registration," in *Proc. 18th ICPR*, vol. 4. Hong Kong, China, 2006, pp. 497–500.
[52] R. O. Duda and P. E. Hart, "Use of the Hough transformation to detect lines and curves in pictures," *Commun. ACM*, vol. 15, no. 1, pp. 11–15, 1972.
[53] D. Ballard, "Generalizing the Hough transform to detect arbitrary shapes," *Pattern Recognit.*, vol. 13, no. 2, pp. 111–122, 1981.
[54] D. G. Lowe, "Distinctive image features from scale-invariant keypoints," *Int. J. Comput. Vis.*, vol. 60, no. 2, pp. 91–110, 2004.
[55] B. Leibe, A. Leonardis, and B. Schiele, "Robust object detection with interleaved categorization and segmentation," *Int. J. Comput. Vis.*, vol. 77, no. 1, pp. 259–289, 2008.
[56] A. Opelt, A. Pinz, and A. Zisserman, "A boundary-fragment-model for object detection," in *Proc. 9th ECCV*, Graz, Austria, 2006, pp. 575–588.
[57] S. Maji and J. Malik, "Object detection using a max-margin Hough transform," in *Proc. 22nd IEEE CVPR*, Miami, FL, USA, 2009, pp. 1038–1045.
[58] O. Barinova, V. Lempitsky, and P. Kholi, "On detection of multiple object instances using Hough transforms," *IEEE Trans. Pattern Anal. Mach. Intell.*, vol. 34, no. 9, pp. 1773–1784, Sep. 2012.
[59] A. Yao, J. Gall, and L. van Gool, "A Hough transform-based voting framework for action recognition," in *Proc. 23rd IEEE CVPR*, San Francisco, CA, USA, 2010, pp. 2061–2068.
[60] L. Kaufman and P. J. Rousseeuw, *Finding Groups in Data: An Introduction to Cluster Analysis*. New York, NY, USA: Wiley, Inc., 1990.
[61] A. Blake, P. Kohli, and C. Rother, *Markov Random Fields for Vision and Image Processing*. Cambridge, MA, USA: MIT Press, 2011.
[62] S. Z. Li, *Markov Random Field Modeling in Image Analysis*, 3rd ed. New York, NY, USA: Springer, 2009.
[63] R. Cappelli, D. Maltoni, and F. Turroni, "Benchmarking local orientation extraction in fingerprint recognition," in *Proc. 20th ICPR*, Istanbul, Turkey, 2010, pp. 1144–1147.
[64] *FVC-OnGoing* [Online]. Available: https://biolab.csr.unibo.it/fvcongoing
[65] J. Feng, Y. Shi, and J. Zhou, "Robust and efficient algorithms for separating latent overlapped fingerprints," *IEEE Trans. Inf. Forensics Security*, vol. 7, no. 5, pp. 1498–1510, Oct. 2012.
[66] *Neurotechnology Inc., VeriFinger* [Online]. Available: http://www.neurotechnology.com
[67] F. Chen, J. Feng, A. K. Jain, J. Zhou, and J. Zhang, "Separating overlapped fingerprints," *IEEE Trans. Inf. Forensics Security*, vol. 6, no. 2, pp. 346–359, Jun. 2011.
[68] Q. Zhao and A. K. Jain, "Model based separation of overlapping latent fingerprints," *IEEE Trans. Inf. Forensics Security*, vol. 7, no. 3, pp. 904–918, Jun. 2012.

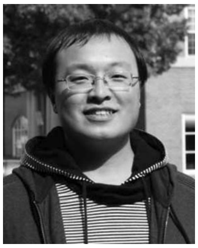

Xiao Yang received the B.S. degree from the Department of Automation, Tsinghua University, Beijing, China, in 2009. Since then, he has been pursuing the Ph.D. degree with i-VisionGroup, Department of Automation, Tsinghua University. His current research interests include fingerprint recognition, palmprint recognition, and computer vision.

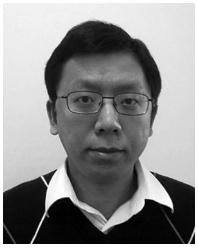

Jianjiang Feng is an associate professor with the Department of Automation, Tsinghua University, Beijing, China. He received the B.S. and Ph.D. degrees from the School of Telecommunication Engineering, Beijing University of Posts and Telecommunications, China, in 2000 and 2007, respectively. From 2008 to 2009, he was a post-doctoral researcher at the Pattern Recognition and Image Processing Laboratory, Michigan State University, East Lansing, MI, USA. His current research interests include fingerprint recognition, palmprint recognition, and structural matching.

Jie Zhou received the B.S. and M.S. degrees from the Department of Mathematics, Nankai University, Tianjin, China, in 1990 and 1992, respectively, and the Ph.D. degree from the Institute of Pattern Recognition and Artificial Intelligence, Huazhong University of Science and Technology (HUST), Wuhan, China, in 1995. From 1995 to 1997, he was a post-doctoral fellow with the Department of Automation, Tsinghua University, Beijing, China. Currently, he is a full professor with the Department of Automation, Tsinghua University. His current research interests include pattern recognition, computer vision, and data mining. In recent years, he has authored over 100 papers in peer-reviewed international journals and conferences. He received the Best Doctoral Thesis Award from HUST in 1995, First Class Science and Technology Progress Award from the Ministry of Education (MOE) in 1998, the Excellent Teaching Award from Tsinghua University, in 2003, and the Best Advisor Awards from Tsinghua University, in 2004 and 2005, respectively. He was selected as one of the outstanding scholars of MOE in 2005. He is an associate editor for the *International Journal of Robotics and Automation and Acta Automatica Sinica*.